Journal of King Saud University – Science 34 (2022) 101851

Contents lists available at ScienceDirect

Journal of King Saud University – Science

journal homepage: www.sciencedirect.com

Original article

Carbon nanotube-coated recombinant human surfactant protein D reduces cell viability in an ovarian cancer cell line, SKOV3, and modulates mTOR pathway and pro-inflammatory cytokine response

Dalal S. Alshaya [a], Areej S. Jalal [a], Najla A. Alburae [b], Nada H. Aljarba [a], Valarmathy Murugaiah [c], Uday Kishore [c], Ahmed A. Al-Qahtani [d,e,*]

[a] Biology Department, College of Science, Princess Nourah bint Abdulrahman University, Riyadh, Saudi Arabia
[b] Biology Department, Faculty of Science, King Abdulaziz University, Jeddah, Saudi Arabia
[c] Biosciences, College of Health and Life Sciences, Brunel University London, Uxbridge UB8 3PH, United Kingdom
[d] Department of Infection and Immunity, Research Centre, King Faisal Specialist Hospital and Research Centre, Riyadh, Saudi Arabia
[e] Department of Microbiology and Immunology, College of Medicine, Alfaisal University, Riyadh, Saudi Arabia

ARTICLE INFO

Article history:
Received 12 September 2021
Revised 22 November 2021
Accepted 18 January 2022
Available online 25 January 2022

Keywords:
Carbon nanotubes
rfhSP-D
Drug delivery
SKOV3
Anti-tumorigenic
Ovarian cancer

ABSTRACT

Nanoparticles such as carbon nanotubes (CNTs) have various clinical and diagnostic applications as utilised for imaging and drug delivery. Therapeutic proteins/peptides can be loaded on CNT coronas to specifically hit immune cells in overdrive or uncontrolled malignant cells. Previously, it was reported that a recombinant version of human surfactant protein D (rfhSP-D) containing trimeric C-type lectin domains induced apoptosis in several tumour cells/cell lines, including SKOV3, which is an ovarian tumour cell line. Solid-phase rfhSP-D coated on a microtiter plate is considerably more potent in inducing apoptosis in breast tumour cells. We have immobilised highly purified, endotoxin-free rfhSP-D on CNTs and assessed its antiproliferative effect on SKOV3 cells. Biotinylated rfhSP-D-CNTs were phagocytosed by SKOV3 cells, followed by apoptosis in a time-dependent manner. Gene expression analysis revealed compromised mTOR complex as a mechanism of apoptosis. When rfhSP-D-CNTs were added to a culture system of SKOV3 cells, it produced a highly proinflammatory immune response that is likely anti-tumorigenic. Thus, rfhSP-D-CNT seems a worthwhile nanocarrier for testing *in vivo* using an animal model of orthotopic ovarian cancer.

1. Introduction

Carbon nanotubes (CNTs) have unique physicochemical attributes, rendering them very useful for biomedical applications. A number of studies have shown that nanoparticles like CNTs offer more efficient means of drug delivery (Bianco et al., 2005; Liu et al., 2009). CNTs are categorized based on their length, diameter, and structure depending on the number of graphene layers from which a single CNT is composed as single-walled CNTs (SWNTs) and multiwalled CNTs (MWCNTs) (Li et al., 2018). Furthermore, MWCNTs were additionally subclassified into double-walled CNTs (DWCNTs) and triple-walled CNTs (TWCNTs) (Kesharwani et al., 2015). MWCNTs are composed of various concentrical layers of graphite with 1–3 nm inner diameter and 2–100 nm of outer diameter (Dresselhaus et al., 1996). Wider inner diameter of MWCNTs offers a greater surface area amenable to high-dose drug loading. Furthermore, the outer walls of MWCNTs can be functionalised by tissue-specific ligands such as antibodies for specific and swift drug delivery.

Understanding the nature of CNTs-immune system interactions is an ideal approach to facilitate their strategic and specific *in vivo* drug delivery (Ali-Boucetta et al., 2008). Many of the key functions of the innate immune system regarding defense against pathogens and synthetic particles such as CNTs, have already been discussed in various studies (Salvador-Morales et al., 2006). For instance, the interaction of phagocytic cells and their surrounding putative receptors with CNTs has been suggested to impact on their

* Corresponding author at: Department of Infection and Immunity, Research Centre, King Faisal Specialist Hospital and Research Centre, Riyadh, Saudi Arabia.
E-mail address: aqahtani@kfshrc.edu.sa (A.A. Al-Qahtani).
Peer review under responsibility of King Saud University.

Production and hosting by Elsevier

https://doi.org/10.1016/j.jksus.2022.101851
1018-3647/

intracellular signalling cascades, thus, the subsequent immune response (Costa et al., 2016). Lungs are a major anatomical site for immuno-therapy with CNTs, and pulmonary toxicity and inflammation is a major concern in using CNTs for treating several diseases, including cancer (Bonner, 2011; Ceppi et al., 2019; Cirillo et al., 2017; Zhang et al., 2012).

Pulmonary surfactant proteins, SP-A and SP-D, are secreted into the alveolar space by epithelial type II cells and have protective effects against pathogens as well as altered self-components such as apoptotic cells and cancer (Haczku, 2008; Kaur et al., 2018a; Kumar et al., 2019; Murugaiah et al., 2020a; Pastva et al., 2007; Thakur et al., 2019). Both these collections opsonize and eliminate pathogens or foreign bodies, and enhance uptake killing through interaction of their putative receptors with alveolar macrophages and activating the immune response (Kishore et al., 2006). Apart from their already well-known functions against pulmonary diseases, the proapoptotic roles of recombinant human SP-D (rfhSP-D) have often been reported against several types of cancers, such as lung, prostate, leukaemia, pancreatic, ovarian and breast cancers (Kaur et al., 2018a; Kumar et al., 2019; Murugaiah et al., 2020a; Thakur et al., 2019). rfhSP-D treatment *in vitro* results in cessation of the cell cycle at G2/M phase, apoptosis, and interferes with metastatic invasion. Meanwhile, the Epidermal Growth Factor (EGF) signalling is also downregulated by SP-D through restriction of EGF-EFGR interactions with human lung adenocarcinoma cells have been found to exhibit decreased proliferation, invasion, and migration (Hasegawa et al., 2015). Cancerous cells that are treated with rfhSP-D show lower Epithelial-Mesenchymal Transition (EMT) through a decrease in transforming growth factor beta (TGF-β) levels, consequently suppressing cell invasion (Kaur et al., 2018b).

In addition to the immune surveillance roles against cancer, SP-A and SP-D are also involved in the processing of inhaled CNTs (Rybak-Smith et al., 2011; Salvador-Morales et al., 2006). Coating oxidised CNTs with SP-A facilitates nanoparticle phagocytosis by alveolar macrophages. Pulmonary surfactant can also stabilize the CNTs in suspensions that are clustered inside macrophages and dendritic cells *in vitro* and *in vivo* (Porter et al., 2009) (Sorensen, 2018).

Ovarian cancer is one of the most fatal forms of female cancer globally with a survival rate of less than 15%, it has become the fifth most common cancer among females (Rogers-Broadway et al., 2016). The prognosis of an early stage ovarian cancer diagnosis compared to later stage cancer with metastasis, is significantly better (Lengyel, 2010). Hence, it is imperative that anticancer therapeutic measures must be designed and developed for the treatment of all types of cancers, including ovarian cancer. This study aims to evaluate the effects of rfhSP-D-CNTs on the ovarian cancer cell line SKOV3, as CNTs are known for their efficient drug delivery mechanism. However, their potential anti-tumour side effects, in conjunction with immune surveillance molecules, have not been thoroughly investigated. Furthermore, this study also aims at investigating the expression of mTOR signalling pathways upon rfhSP-D-CNT treatment, since mTOR pathway is frequently detected in ovarian cancers (Altomare et al. 2004). Previously, studies have reported that ovarian cancer cells, including SKOV3 cell line, exhibit the trigger of Akt/mTOR pathway, thus, protecting the tumour cells from induction of apoptosis (Peng et al. 2010).

2. Methods and materials

2.1. Dispersion and functionalization of CNTs

CNTs (diameters 10–20 nm, length 5–20 μm) were obtained from Arry Nano (Frechen Königsdorf, Germany). A combination of sulfuric acid with nitric acid in a ratio of 3:1 was used for CNT dispersion through sonication on ICE. Whereas, whereas the same was functionalized with Carboxymethyl Cellulose (CMC, Sigma) in a mass ratio of 1:2 (Pondman et al., 2015) by probe sonication. Aggregates and clusters were removed via centrifugation at 8000g, followed by washing out the excess CMC using a polycarbonate track-etched membrane filter (0.2 μm) (Whatman). For covalent functionalization, the acidic mixture was refluxed for 48 h at 120 °C.

2.2. Expression and purification of rfhSP-D

The procedure for expressing and purifying the recombinant form of truncated human SP-D (rfhSP-D) was defined previously (Kaur et al., 2018a; Murugaiah et al., 2020a). As reported previously, pUK-D1 plasmid (composed of cDNA sequences for 8 Gly-X-Y repeats, α-helical neck, and CRD region of human SP-D) was transformed in Escherichia coli BL21 (λDE3) pLysS bacterial strain (Invitrogen). 25 ml of primary bacterial inoculum was inoculated in 500 ml of Luria-Bertani (LB) medium containing 34 μg/ml chloramphenicol and 100 μg/ml ampicillin (Sigma-Aldrich) and grown until the OD600 of 0.6. The grown bacterial cells were then induced with isopropyl β-D-1-thiogalactopyranoside (IPTG) (0.5 mM) for 3 h hours on a shaker at 37 °C following IPTG-induction, the bacterial cells were lysed in buffer containing 50 mM Tris–HCl pH 7.5, 200 mM NaCl, 5 mM EDTA pH 8, 0.1% v/v Triton X-100, 0.1 mM phenyl-methyl-sulfonyl fluoride, 50 μg/ml lysozyme). The lysed cells were then sonicated (five cycles, 30 s each) and centrifuged for 30 min at 12,000×g. The inclusion bodies containing inactive form of rfhSP-D were subjected to denaturation and renaturation process using refolding buffer (50 mM Tris–HCl pH 7.5, 100 mM NaCl, 10 mM 2-mercaptoethanol) containing 8 M urea. The dialysate was then passed onto a maltose-agarose column (5 ml; Sigma-Aldrich) and rfhSP-D was eluted using 10 mM EDTA buffer. Affinity purified rfhSP-D was then subjected to endotoxin levels using QCL-1000 Limulus amebocyte lysate system (Lonza). Affinity purified rfhSP-D was set to release from LPS down to the level of ~5 pg/μg of rfhSP-D.

2.3. Sodium dodecyl sulfate polyacrylamide gel electrophoresis (SDS-PAGE)

The purity of rfhSP-D fractions, or the bonding of rfh-SPD with CMC-CNTs was evaluated using a 12% vol/vol SPD-PAGE gel. Protein samples were mixed with 2X sample buffer and denatured by heating at 95 °C for ten minutes before being applied to the gels. A standard prestained protein marker (by Fischer-Scientific) was also loaded on the gel for evaluating purified rfhSP-D size. Staining solution was prepared from 1 g Sigma-Aldrich Brilliant Blue, 50% v/v solution of methanol (Fischer-Scientific), 10% vol/vol solution of Acetic Acid (Fischer-Scientific), and 40 ml distilled water. It was then used to stain the SDS-PAGE gel for about 2 h. The stained gel was afterward destained by using a mixture of 40% vol/vol solution of methanol and 10% vol/vol solution of Acetic Acid until the time protein bands became visible.

2.4. Western blotting

Western blotting approach was used to identify and establish the immuno-reactivity of rfhSP-D. For this purpose, 10 μg of rfhSP-D were resuspended in 10 μl of 2X loading buffer solution, and the suspension was subsequently brought to boil at 100 °C for 15 min, with BSA as a negative control protein. After being run on 12% SDS-PAGE, samples were then transferred through a 230 mA nitrocellulose membrane (Sigma-Aldrich) for 2 h in a transfer buffer. A 5% wt/vol solution of dried milk powder, PBS

was used to block the membrane for 2 h at 4 °C. Later, after washing, rabbit anti-human SP-D primary antibody (1:1000) was used for the probing of the membrane, subsequently followed by a secondary 1:1000 conjugate of goat anti-rabbit IgG horseradish peroxidase (HRP) for 1 h at room temperature. A 3′-diaminobenzidine (DAB) substrate kit was used to develop color.

2.5. Coupling of rfhSP-D to non-Covalently with carboxymethylcellulose (CMC-CNT)

About 20 μg/ml of rfhSP-D with CMC-CNT in a ratio of 2:1 was incubated overnight at 4 °C, with 5 mM Calcium Chloride. This was followed by washing in PBS, then centrifugation at 15,000×g to remove unbound proteins. rfhSP-D bound to CMC-CNT was analysed with SDS-PAGE.

2.6. Cell culture and treatments

SKOV3 (ATCC, USA) is a human ovarian clear cell with adenocarcinoma cell line. A complete DMEM-F12 medium was applied for cell culture, which was supplemented with foetal calf serum (10% v/v), L-glutamine (2 mM), and penicillin (100 U/ml)/streptomycin (100 μg/ml) (Thermo Fisher). The cells were grown at 37 °C and 5% CO2 until they were between 80 to 90% confluent. For washing of the cells, PBS was utilized. SKOV3 cells were seeded on six-well plates and treated with rfhSP-D-CNT at various time points.

2.7. CNT uptake assay

CMC-CNTs were biotinylated using 0.1 M MES with 1 mg pentylamine biotin (Pierce) together with 4 μg EDC (1-Ethyl-3-(3-dimethylaminopropyl) carbodiimide) and buffer for 2 h. This was stopped by the addition of 0.1 M ethanolamine and dialysed overnight against PBS. Using Alexa Fluor 488-conjugated Streptavidin, biotinylated CNTs were incubated for 30 min.

2.8. MTT assay

SKOV3 cells (0.1×10^5) were seeded in a 96-well microtiter plate and incubated with rfhSP-D-CNT (5, 10, and 20 μg) in serum-free DMEM-F12 medium for 24 h or 48 h. After removal of the medium and cell washing with PBS, MTT [3-(4,5-dimethylthiazol-2-yl)-2,5-diphenyltetrazolium bromide] (100 μl/well; 5 mg/ml stock) was added to the cells and incubated for 4 h at 37 °C. Cells were incubated at 37 °C for 10 min after the removal of 75 μl of medium, while 50 μl of dimethyl sulfoxide was added up to each well. The absorbance was read at 570 nm using a plate reader.

2.9. Quantitative Real-Time Polymerase Chain Reaction (RT-PCR)

SKOV3 (0.4×10^6) cells with rfhSP-D-CNT (5, 10, and 20 μg) were grown in serum-free DMEM-F12 medium at various time points. RNA was isolated using Total RNA Purification Kit (Sigma-Aldrich), following manufacturer's instructions. For the synthesis of cDNA, an isolated 2 μg RNA were utilized (Applied Biosystems). With the help of Primer-BLAST software, primer sequences were designed (Table 1). Each PCR was performed in triplicate and each reaction included SYBR Green MasterMix (5 μl) (Applied Biosystems), primers (75 nM), and cDNA (500 ng) (7900HT; Applied Biosystems). The cycle involved 2′/50 °C and 10′/95 °C, and then 40 cycles (15 s/95 °C; 1′/60 °C). Human 18S rRNA was applied as a housekeeping control. For the calculation of the relative expression of each target, the $2-\Delta\Delta Ct$ formula for relative quantification (RQ) was used.

$$RQ = 2 - \Delta\Delta Ct$$

2.10. Multiplex cytokine array analysis

Secreted cytokines: IL-6, IL-10, IL12p40, IL12p70, IL-1α, IL-1β, TNF-α, IL-15, IL-17A, IL-9, TNF-β, IFN-α2; chemokines: MCP-3, MDC, Eotaxin, Fractalkine, GRO, IL-8, IP-10, MCP-1, MIP-1α, MIP-1β, MIG, I-TAC, MIG; growth factors: IL-9, IL-2, EGF, FGF-2, G-CSF, GM-CSF, IL-3, IL-7, VEGF; and ligand and receptors: FLT-3L, IL-1RA, sCD40L were measured by MagPix Milliplex kit (EMD Millipore), as reported previously (Pondman et al., 2015).

2.11. Statistical analysis

The GraphPad Prism 6.0 software was applied for graphical presentation. To check the level of significance and differences between untreated and treated samples, a one-way analysis of variance (ANOVA) test was used; the p-values $^*p < 0.05$, $^{**}p < 0.01$, and $^{***}p < 0.001$ were set. The standard deviation (SD) and standard error of the mean (SEM) were presented using error bars (n = 3).

3. Results

3.1. Expression, purification, and binding of rfhSP-D to CMC-CNTs

The rfhSP-D, containing eight Gly-X-Y triplets, neck domain and lectin domain, was expressed as inclusion bodies, migrating at ~20 kDa under reducing conditions (Fig. 1A). SP-D rabbit/anti-human polyclonal primary antibody recognised rfhSP-D on western blot. Various concentration of rfhSP-D, that is, 5, 10, or 20 μg/ml, was used for the incubation of CMC-CNTs in 1:2 wt rations. After incubation, the results showed purified LPS-free rfhSP-D was stably attached to CMC-CNT (Fig. 2).

3.2. CNT-rfhSP-D binds SKOV3 cell line and reduces cell viability

The MTT assay was used for quantitative analysis of rfhSP-D-CNT and CNT cell viability that were only treated with SKOV3 at 24 h and 48 h (Fig. 3). The incubation of cells was carried out with rfhSP-D-CNT in a concentration of 5, 10, or 20 μg/ml along with CNT control in a serum-free DMEM-F12 medium, where no protein was coated. MTT data showed that cell viability was significantly reduced after incubation with rfhSP-D-CNT for 48 h (Fig. 3). It

Table 1
Target genes and primers used in the qPCR analysis.

Target Gene	Forward Primers	Reverse Primers
18S	5′-ATGGCCGTTCTTAGTTGGTG-3′	5′-CGCTGAGCCAGTCAGTGTAG-3′
mTOR	5′-TGCCAACTATCTTCGGAACC-3′	5′-GCTCGCTTCACCTCAAATTC-3′
RICTOR	5′-GGAAGCCTGTTGATGGTGAT-3′	5′-GGCAGCCTGTTTTATGGTGT-3′
RAPTOR	5′-ACTGATGGAGTCCGAAATGC-3′	5′-TCATCCGATCCTTCATCCTC-3′

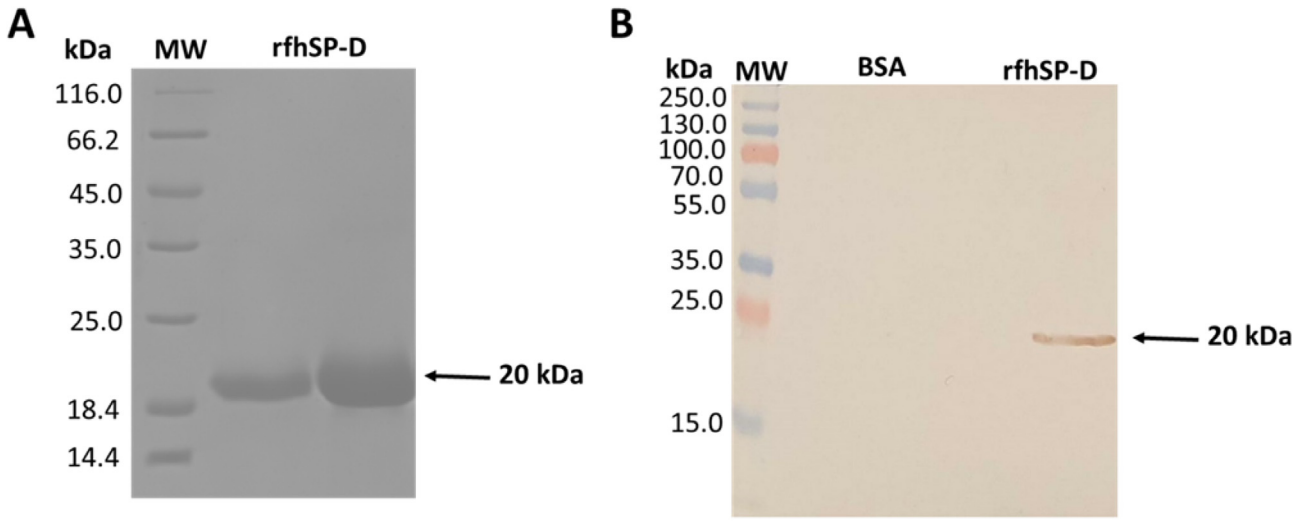

Fig. 1. Immuno-blot proofing of reduced rfhSP-D with purified affinity and a 12% vol/vol solution of SDS-PAGE. (A) Urea based denaturisation was used to capture rfhSP-D proteins, migrating at approximately 20 kDa. Subsequent purification of properly folded rfhSP-D, eluted by EDTA, was done with maltose agarose. (B) Application of western blotting approach with the use of rabbit/anti-human SP-D polyclonal primary antibody. Figure shows the immuno-reactivity of purified rfhSP-D protein. Lane 1 shows the negative control Sample (BSA), while lane 2 depicts 10 μg/well of purified rfhSP-D.

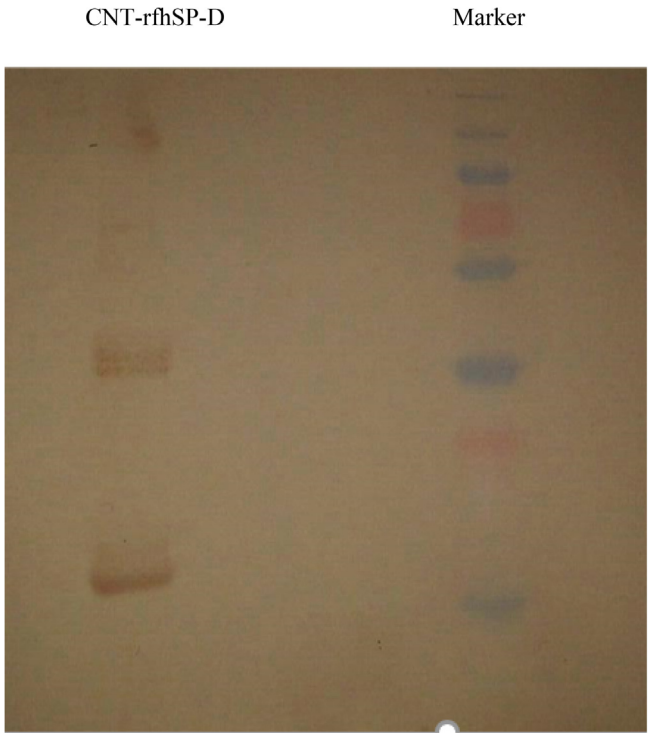

Fig. 2. Binding of rfhSP-D to CMC-CNT. Analysis of rfhSP-D with 12% wt/vol SDS-PAGE solution. CMC-CNTS were incubated overnight along with purified rfhSP-D, in a weight ratio of 1:2. They were washed with PBS afterwards and then put into a centrifuge to remove all free rfhSP-D. The first lane in the figure shows the molecular weight marker, while the second lane shows CMC-CNT – rfhSP-D. Monomeric, dimeric, and trimeric protein chains can also be seen in lane 2.

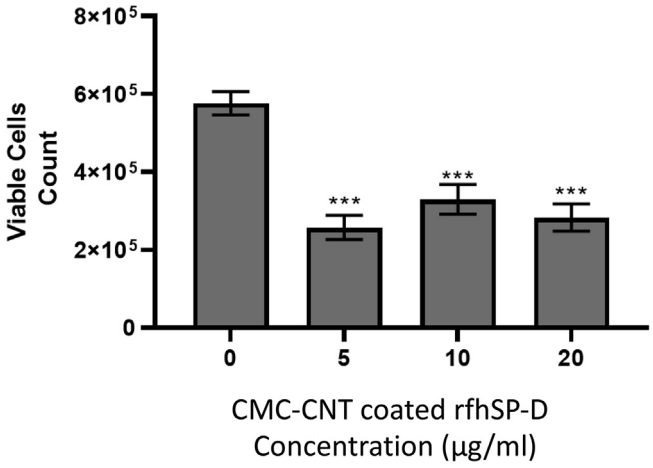

Fig. 3. Use of MTT Assay to show the reduction in cell viability by rfhSP-D bound with CMC-CNT in SKOV3 ovarian cancer line. Multiple concentrations of CMC-CNT bound rfhSP-D (0, 5, 10, and 20 μg/ml) were used to treat these SKOV3 cells (0.1×10^5), along with an untreated control sample. They were incubated at 37 °C for 48 h under standard conditions for cell culture. The assays were performed in groups of three ± SEM. One-way unpaired ANOVA was carried out between untreated cells and cells treated with rfhSP-D bound with CMC-CNT. P-value at n = 3 was found to be <0.001.

was found around ~50% cell viability reduction was seen among all concentrations tested at 48 h (Fig. 3).

3.3. Down-regulation of RICTOR and RAPTOR by CNT-rfhSP-D

The expression of mTOR signalling pathways were also investigated in this study as it is often found in ovarian tumours. The mRNA expressions of prosurvival factors, including RICTOR (Fig. 4B), and RAPTOR (Fig. 4C) were significantly downregulated (approximately ~log10 −1-fold) at 6 hours, indicating that rfhSP-D-CNTs can downregulate mTOR signalling shortly just after the treatment. Thus, shuttling of these mTOR components may lead to dysregulation of the downstream signalling cascade (i.e., dephosphorylation of S6K), and hence, subsequently, inhibit the proliferation of cells.

3.4. Cytokine expression by SKOV3 cells treated with rfhSP-D-CNT

Multiplex cytokines, growth factors, chemokines, and soluble ligands were measured in the supernatant after the treatment of SKOV3 cells along with CNTs or rfhSP-D-CNTs at 24 and 48-hour time points. Out of the various analytes examined, as mentioned

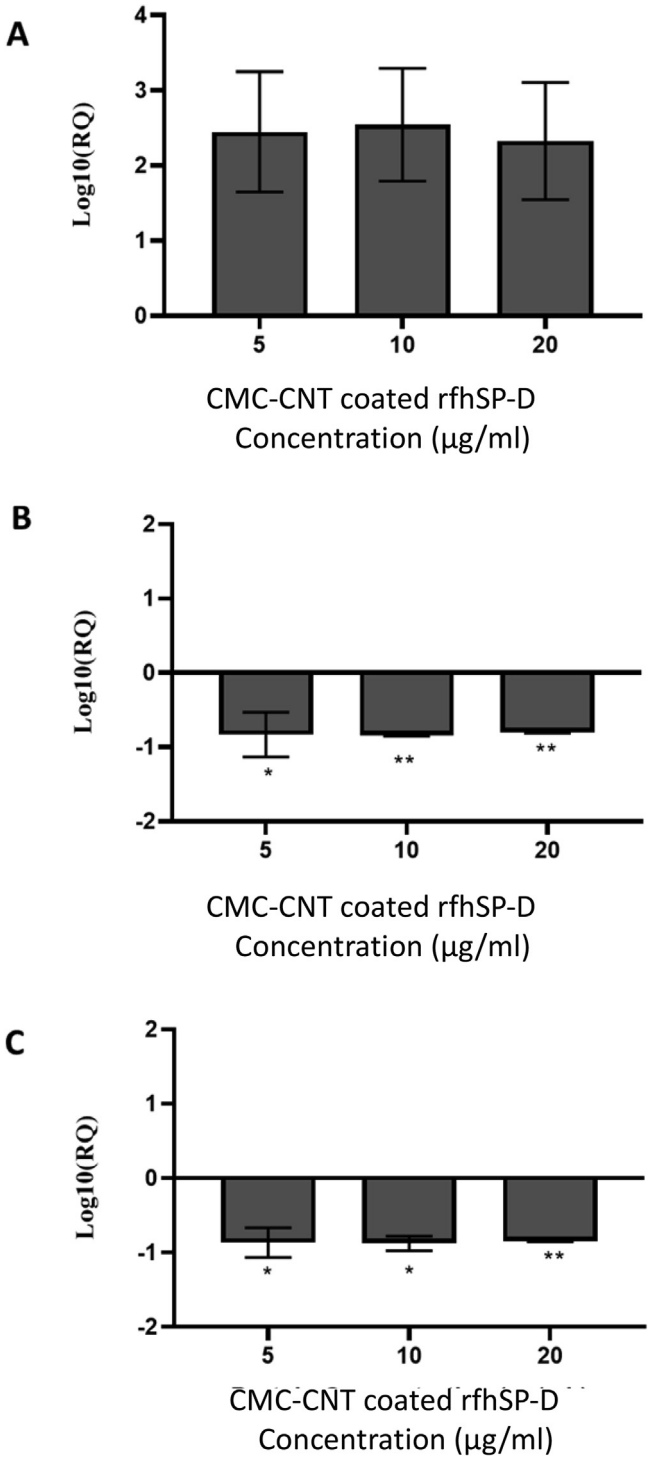

Fig. 4. Comparison of relative quantification of mammalian rapamycin (mTOR). A = RAPTOR. B = RICTOR. C = mRNA expression in SKOV3 cells that were treated with rfhSP-D-CNT at multiple concentrations (as described in Fig. 3 description) for 6 h, in conjunction with CNT alone as a control. rfhSP-D-CNT (0, 5, 10, or 20 µg/ml) was used to seed SKOV3 (0.4×10^6) cells, while both, CNT and rfhSP-D treated cells were used for cDNA synthesis, qPCR and for total RNA extraction using 18S rRNA as a housekeeping control. Assays were performed in groups of three, with error bars represented as ± SEM. Significance of correlation between untreated and rfhSP-D-CNT treated cells was evaluated using the unpaired one-way ANOVA test [$^{*}p < 0.05$ and $^{**}p < 0.01$ (n = 3)].

in the Methods section, only IL-β1, TNF-α, TGF-β, and GM-CSF were detectable at reasonable levels (Fig. 5). Other analytes were at the base level, and hence not shown here. rfhSP-D-CNTs in general increased the levels of proinflammatory cytokines at 24 h as well as 48 h (Fig. 5).

4. Discussion

CNTs have been proposed as promising therapeutic vehicles (nanocarriers). Concomitantly, rfhSP-D, via several recent studies, has been shown to reduce the proliferation of various cancer cell lines via a diverse range of cellular and molecular mechanisms (Kaur et al., 2018a; Kaur et al., 2018b; Kumar et al., 2019; Murugaiah et al., 2020a; Thakur et al., 2019; Thakur et al., 2020). Thus, it is important to understand the dynamic nature of cellular and molecular interactions involving CNTs with rfhSP-D to develop nanocarriers for future preclinical trials.

The calcium-dependent collectins, SP-A and SP-D, act as molecular pattern recognition innate immune molecules. SP-D induces a robust proinflammatory reaction following its interaction with pathogens (Kishore et al., 2006; Murugaiah et al., 2020b). SP-D primary structure has a characteristic N-terminal region, collagen region, and neck region, followed by a C-terminal C-type lectin or carbohydrate recognition domain (CRD) (Kishore et al., 2006). In the current study, rfhSP-D expressed in *E. coli*, was used, consisting of three CRDs, which shows a number of biological properties similar to collagen-containing full-length SP-D (Kishore et al., 2006). SP-D behaves like an opsonin and enhances phagocytosis, a superoxidative burst, in addition to a proinflammatory immune response by phagocytic cells (Murugaiah et al., 2020b). In addition to enhancing phagocytosis via opsonization, SP-D was also found to directly trigger and stimulate phagocytosis, by the upregulating the cell surface phagocytic receptors present on macrophages, without the requirement for microbial binding. This has been demonstrated for the mannose receptor found on monocyte-derived macrophages, where SP-D was found to up-regulate its activity Beharka et al., 2002; Kudo et al., 2004). These properties of SP-D have been validated *in vivo* using SP-D gene knock-out mice, which showed highly inflamed lungs (Madan et al., 2005).

An important anti-tumour role of SP-D (as along with rfhSP-D in most cases) has been recently unearthed, raising the possibility that it behaves as an immune surveillance targeting tumour cells. Recently, it has also been reported that these protein D (rfhSP-D) induce apoptosis in highly aggressive pancreatic tumours (Kaur et al., 2018a) and epithelial-to-mesenchymal transition via TGF-β mediated intervention (Kaur et al., 2018b). Similarly, some studies using cancer and breast cancer cell lines found the same results (including androgen-resistant prostate cancer cell lines) (Thakur et al., 2019; Thakur et al., 2020). These studies have also delineated various apoptotic pathways involved in the induction of apoptosis. One experiment that is of great importance is that solid-phase rfhSP-D was by far the most efficient in inducing apoptosis in breast cancer cells compared to solution-phase rfhSP-D (Murugaiah et al., 2020a). Thus, it appears that rfhSP-D immobilised on solid phase such as nanocarriers (including CNTs for example) is likely to be more potent in inducing apoptosis in target tumour cells.

SP-D has been shown to interact with EGF receptor on A549 cell line and interfere with its interaction with EGF, thus, leads to suppression of lung cancer progression (Hasegawa et al., 2015). rfhSP-D was found to interact with eosinophilic leukemic and prostate cancer cells via its CRD (Mahajan et al., 2013). The SPD-CRD complex is known to bind and interact with TLR-2, TLR-4, CD14, EGFR and SIRPα that are reported to be present on various cancer cells (Hasegawa et al., 2015; Mahajan et al., 2013; Ohya et al., 2006; Janssen et al., 2008). Furthermore, rfhSP-D binding to its pattern recognition recepors, including CD14, TLR-2 and TLR-4 may result

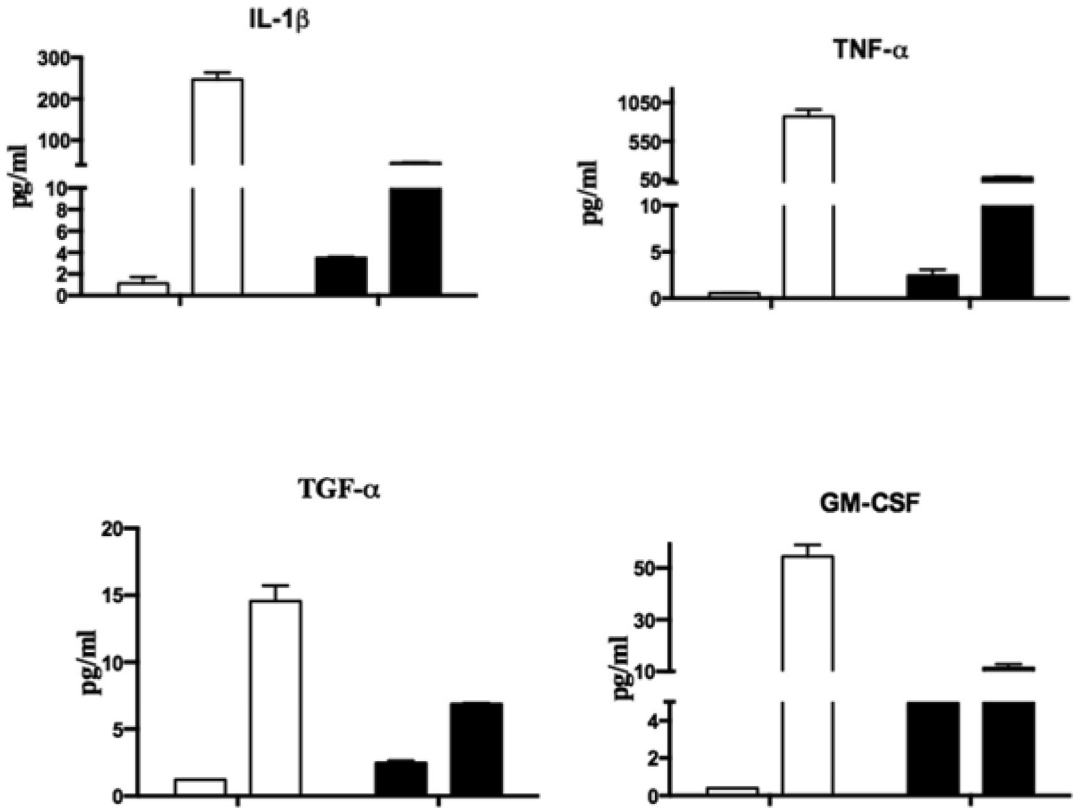

Fig. 5. MCA (Multiple Cytokine Array) Analysis of SKOV3 cells' supernatants with CNT along and rfhSP-D-CNT. rfhSP-D-CNTs and SKOV3 cells incubated for 24 and 48 h. Protein levels of secreted cytokines, chemokines, growth factors, and other ligands and receptors were measured by taking culture supernatants at late time points (24 h and 48 h), using a cytokine array, as listed in the Methods section of this article. Incubation periods, both 24 and 48 h, were plotted on the x-axis. Error bars show the ± standard deviation. A 2-way ANOVA showed significant differences ($p < 0.05$) in expression between rfhSP-D-CNTs and CNTs alone.

in blockade of their pro-survival and pro-inflammatory downstream pathways (Thakur et al., 2019).

The rfhSP-D expressed by *E. coli* was used in this study under T7 promoter as inclusion bodies and purified to homogeneity using denaturation-renaturation cycle and affinity chromatography. We then immobilised highly purified, endotoxin-free rfhSP-D on CMC-CNTs and tested its ability to induce an antiproliferative effect on SKOV3 cells via MTT assay. Biotinylated rfhSP-D-CNTs were taken up by SKOV3 cells triggering apoptosis in the target cells in a time-dependent manner. This assessment was based on a cell viability assay. SKOV-3 is a hypodiploid human cell line with HER-2^+ genotyping, and SKOV-3 cells are resistant to tumour necrosis factor and to several cytotoxic drugs including diphtheria toxin, *cis*-platinum and adriamycin. In this context, it was worthwhile examining the pro-apoptotic effects of rfhSP-D in these cells, since rfhSP-D was shown to induce apoptosis in other cancer cells.

The mTOR pathway is an important survival pathway for cell growth, metabolism, gene expression and protein synthesis (Gentilella et al. 2015). mTOR pathway functions through two distinct protein complexes, known as mTORC1 (Raptor) and mTORC2 (Rictor) (Beauchamp and Platanias, 2013). In this context, given the pro-apoptotic potential of rfhSP-D treatment, this study was also aimed at examining the effect of rfhSP-D-CNT treatment on mTOR signalling pathway. The apoptotic pathway involved a compromised mTOR complex, examining the mTOR key players, as revealed by qPCR. qPCR results showed that treatment with rfhSP-D-CNT had a profound effect on mTOR, DEPTOR, and Rictor. At 24 h, the expression of mTOR and DEPTOR was upregulated, with rfhSP-D-CNT treatment having a more profound effect on DEPTOR mRNA expression. Regarding Rictor and Raptor transcript expression, rfhSP-D-CNT treatment resulted in a decrease of both genes. The protein interactions in both mTOR complexes (mTORC1 and mTORC2) may have been compromised with reduced expression of Rictor and Raptor, resulting in the downregulation of the mTOR pathway. The compromised interaction between the factors in the mTOR pathway may thus be responsible for the reduced cell viability observed through inhibition of protein synthesis, cell growth and proliferation.

When rfhSP-D-CNTs were added to cultured SKOV3 cells, it induced a high proinflammatory response that is likely to be anti-tumorigenic. Of note is the upregulation of proapoptotic TNF-α that has been implicated in the pathways leading to apoptotic cell death in SKOV3 cells (Kaur et al., 2016). In conclusion, rfhSP-D bound to CMC-CNTs can be taken up by SKOV3 cells, which in turn reduces the viability of the cultured SKOV3 cells. This reduction in cell viability (apoptosis induction) is likely to be engineered by a compromised mTOR pathway and enhanced death mechanisms via TNF-α. Thus, rfhSP-D-CNT seems a worthwhile nanocarrier for testing *in vivo* in a murine model of orthotopic ovarian cancer.

Declaration of Competing Interest

The authors declare that they have no known competing financial interests or personal relationships that could have appeared to influence the work reported in this paper.

Acknowledgements

This research was funded by the Deanship of Scientific Research at Princess Nourah bint Abdulrahman University, Riyadh, KSA, through the Research Funding Program (Grant No# FRP-1440-27).

References

Ali-Boucetta, H., Al-Jamal, K.T., McCarthy, D., Prato, M., Bianco, A., Kostarelos, K., 2008. Multiwalled carbon nanotube-doxorubicin supramolecular complexes for cancer therapeutics. Chem. Commun. (Camb.) (4), 459–461. https://doi.org/10.1039/B712350G.

Altomare, D.A., Wang, H.Q., Skele, K.L., De Rienzo, A., Klein-Szanto, A.J., Godwin, A.K., et al., 2004. AKT and mTOR phosphorylation is frequently detected in ovarian cancer and can be targeted to disrupt ovarian tumor cell growth. Oncogene 23 (34), 5853–5857. https://doi.org/10.1038/sj.onc.1207721.

Beauchamp, E.M., Platanias, L.C., 2013. The evolution of the TOR pathway and its role in cancer. Oncogene 32, 3923–3932. https://doi.org/10.1038/onc.2012.567.

Beharka, A.A., Gaynor, C.D., Kang, B.K., Voelker, D.R., McCormack, F.X., Schlesinger, L. S., 2002. Pulmonary surfactant protein A upregulates activity of the mannose receptor, a pattern recognition receptor expressed on human macrophages. J. Immunol. 169 (7), 3565–3573.

Bianco, A., Kostarelos, K., Partidos, C.D., Prato, M., 2005. Biomedical applications of functionalised carbon nanotubes. Chem. Commun. (Camb.) (5), 571. https://doi.org/10.1039/b410943k.

Bonner, J.C., 2011. Carbon nanotubes as delivery systems for respiratory disease: do the dangers outweigh the potential benefits? Expert. Rev. Respir. Med. 5 (6), 779–787.

Ceppi, L., Bardhan, N.M., Na, Y.J., Siegel, A., Rajan, N., Fruscio, R., Del Carmen, M.G., Belcher, A.M., Birrer, M.J., 2019. Real-time single-walled carbon nanotube-based fluorescence imaging improves survival after debulking surgery in an ovarian cancer model. ACS Nano 13 (5), 5356–5365.

Cirillo, G., Di Pino, G., Capone, F., Ranieri, F., Florio, L., Todisco, V., Tedeschi, G., Funke, K., Di Lazzaro, V., 2017. Neurobiological after-effects of non-invasive brain stimulation. Brain Stimul. 10 (1), 1–18.

Costa, P.M., Bourgognon, M., Wang, J.-W., Al-Jamal, K.T., 2016. Functionalised carbon nanotubes: From intracellular uptake and cell-related toxicity to systemic brain delivery. J. Control. Release 241, 200–219.

Dresselhaus, M., Dresselhaus, G., Eklund, P., 1996. Science of Fullerenes and Carbon Nanotubes: Their Properties and Applications. Elsevier, San Diego, CA, USA.

Gentilella, A., Kozma, S.C., Thomas, G., 2015. A liaison between mTOR signaling, ribosome biogenesis and cancer. Biochim. Biophys. Acta, Gene Regul. Mech. 1849, 812–820. https://doi.org/10.1016/j.bbagrm.2015.02.005.

Haczku, A., 2008. Protective role of the lung collectins surfactant protein A and surfactant protein D in airway inflammation. J. Allergy Clin. Immunol. 122 (5), 861–879.

Hasegawa, Y., Takahashi, M., Ariki, S., Asakawa, D., Tajiri, M., Wada, Y., Yamaguchi, Y., Nishitani, C., Takamiya, R., Saito, A., Uehara, Y., Hashimoto, J., Kurimura, Y., Takahashi, H., Kuroki, Y., 2015. Surfactant protein D suppresses lung cancer progression by downregulation of epidermal growth factor signaling. Oncogene 34 (7), 838–845.

Janssen, W.J., McPhillips, K.A., Dickinson, M.G., Linderman, D.J., Morimoto, K., Xiao, Y.Q., et al., 2008. Surfactant proteins A and D suppress alveolar macrophage phagocytosis via interaction with SIRP alpha. Am. J. Respir. Crit. Care Med. 178, 158–167. https://doi.org/10.1164/rccm.200711-1661OC.

Kaur, A., Riaz, M.S., Murugaiah, V., Varghese, P.M., Singh, S.K., Kishore, U., 2018a. A recombinant fragment of human surfactant protein D induces apoptosis in pancreatic cancer cell lines via Fas-mediated pathway. Front. Immunol. 9, 1126.

Kaur, A., Riaz, M.S., Singh, S.K., Kishore, U., 2018b. Human surfactant protein D suppresses epithelial-to-mesenchymal transition in pancreatic cancer cells by downregulating TGF-beta. Front. Immunol. 9, 1844.

Kaur, A., Sultan, S.H., Murugaiah, V., Pathan, A.A., Alhamlan, F.S., Karteris, E., Kishore, U., 2016. Human C1q induces apoptosis in an ovarian cancer cell line via tumor necrosis factor pathway. Front. Immunol. 7, 599.

Kesharwani, P., Mishra, V., Jain, N.K., 2015. Validating the anticancer potential of carbon nanotube-based therapeutics through cell line testing. Drug Discov. Today 20 (9), 1049–1060.

Kishore, U., Greenhough, T.J., Waters, P., Shrive, A.K., Ghai, R., Kamran, M.F., Bernal, A.L., Reid, K.B.M., Madan, T., Chakraborty, T., 2006. Surfactant proteins SP-A and SP-D: structure, function and receptors. Mol. Immunol. 43 (9), 1293–1315.

Kudo, K., Sano, H., Takahashi, H., Kuronuma, K., Yokota, S.-I., Fujii, N., Shimada, K.-I., Yano, I., Kumazawa, Y., Voelker, D.R., Abe, S., Kuroki, Y., 2004. Pulmonary collectins enhance phagocytosis of Mycobacterium avium through increased activity of mannose receptor. J. Immunol. 172 (12), 7592–7602.

Kumar, J., Murugaiah, V., Sotiriadis, G., Kaur, A., Jeyaneethi, J., Sturniolo, I., Alhamlan, F.S., Chatterjee, J., Hall, M., Kishore, U., Karteris, E., 2019. Surfactant protein D as a potential biomarker and therapeutic target in ovarian cancer. Front. Oncol. 9, 542.

Lengyel, E., 2010. Ovarian cancer development and metastasis. Am. J. Pathol. 177 (3), 1053–1064.

Li, W., Tierce, N.T., Bekyarova, E., Bardeen, C.J., 2018. Protection of molecular microcrystals by encapsulation under single-layer graphene. ACS Omega 3 (7), 8129–8134.

Liu, Z., Tabakman, S., Welsher, K., Dai, H., 2009. Carbon nanotubes in biology and medicine: in vitro and in vivo detection, imaging and drug delivery. Nano Res. 2 (2), 85–120.

Madan, T., Reid, K.B.M., Singh, M., Sarma, P.U., Kishore, U., 2005. Susceptibility of mice genetically deficient in the surfactant protein (SP)-A or SP-D gene to pulmonary hypersensitivity induced by antigens and allergens of Aspergillus fumigatus. J. Immunol. 174 (11), 6943–6954.

Murugaiah, V., Agostinis, C., Varghese, P.M., Belmonte, B., Vieni, S., Alaql, F.A., Alrokayan, S.H., Khan, H.A., Kaur, A., Roberts, T., Madan, T., Bulla, R., Kishore, U., 2020a. Hyaluronic acid present in the tumor microenvironment can negate the pro-apototic effect of a recombinant fragment of human surfactant protein D on breast cancer cells. Front. Immunol. 11, 1171.

Murugaiah, V., Tsolaki, A.G., Kishore, U., 2020b. Collectins: innate immune pattern recognition molecules. Adv. Exp. Med. Biol. 1204, 75–127.

Ohya, M., Nishitani, C., Sano, H., Yamada, C., Mitsuzawa, H., Shimizu, T., Saito, T., Smith, K., Crouch, E., Kuroki, Y., 2006. Human pulmonary surfactant protein D binds the extracellular domains of Toll-like receptors 2 and 4 through the carbohydrate recognition domain by a mechanism different from its binding to phosphatidylinositol and lipopolysaccharide. Biochemistry 45 (28), 8657–8664. https://doi.org/10.1021/bi060176z.

Pastva, A.M., Wright, J.R., Williams, K.L., 2007. Immunomodulatory roles of surfactant proteins A and D: implications in lung disease. Proc. Am. Thorac. Soc. 4 (3), 252–257.

Peng, D., Wang, J., Zhou, J., Wu, G.S., 2010. Role of the Akt/mTOR survival pathway in cisplatin resistance in ovarian cancer cells. Biochem. Biophys. Res. Commun. 394 (3), 600–605. https://doi.org/10.1016/j.bbrc.2010.03.029.

Pondman, K.M., Pednekar, L., Paudyal, B., Tsolaki, A.G., Kouser, L., Khan, H.A., Shamji, M.H., ten Haken, B., Stenbeck, G., Sim, R.B., Kishore, U., 2015. Innate immune humoral factors, C1q and factor H, with differential pattern recognition properties, alter macrophage response to carbon nanotubes. Nanomedicine 11 (8), 2109–2118.

Porter, A.E., Gass, M., Bendall, J.S., Muller, K., Goode, A., Skepper, J.N., Midgley, P.A., Welland, M., 2009. Uptake of noncytotoxic acid-treated single-walled carbon nanotubes into the cytoplasm of human macrophage cells. ACS Nano 3 (6), 1485–1492.

Rogers-Broadway, K.R., Chudasama, D., Pados, G., Tsolakidis, D., Goumenou, A., Hall, M., Karteris, E., 2016. Differential effects of rapalogues, dual kinase inhibitors on human ovarian carcinoma cells in vitro. Int. J. Oncol. 49, 133–143.

Rybak-Smith, M.J., Pondman, K.M., Flahaut, E., Salvador-Morales, C., Sim, R.B., 2011. Recognition of Carbon Nanotubes by the Human Innate Immune System, in: R. Klingeler, R.B.S.E. (Ed.), Carbon nanotubes for biomedical applications (Carbon nanostructures). Springer, pp. 183-210.

Salvadormorales, C., Flahaut, E., Sim, E., Sloan, J., Hgreen, M., Sim, R., 2006. Complement activation and protein adsorption by carbon nanotubes. Mol. Immunol. 43 (3), 193–201.

Sorensen, G.L., 2018. Surfactant protein D in respiratory and non-respiratory diseases. Front. Med. (Lausanne) 5, 18.

Thakur, G., Prakash, G., Murthy, V., Sable, N., Menon, S., Alrokayan, S.H., Khan, H.A., Murugaiah, V., Bakshi, G., Kishore, U., Madan, T., 2019. Human SP-D acts as an innate immune surveillance molecule against androgen-responsive and androgen-resistant prostate cancer cells. Front. Oncol. 9, 565.

Thakur, G., Sathe, G., Kundu, I., Biswas, B., Gautam, P., Alkahtani, S., Idicula-Thomas, S., Sirdeshmukh, R., Kishore, U., Madan, T., 2020. Membrane interactome of a recombinant fragment of human surfactant protein D reveals GRP78 as a novel binding partner in PC3, a metastatic prostate cancer cell line. Front. Immunol. 11. https://doi.org/10.3389/fimmu.2020.600660.

Zhang, W., Zhang, D., Tan, J., Cong, H., 2012. Carbon nanotube exposure sensitize human ovarian cancer cells to paclitaxel. J. Nanosci. Nanotechnol. 12 (9), 7211–7214.